Accepted Manuscript

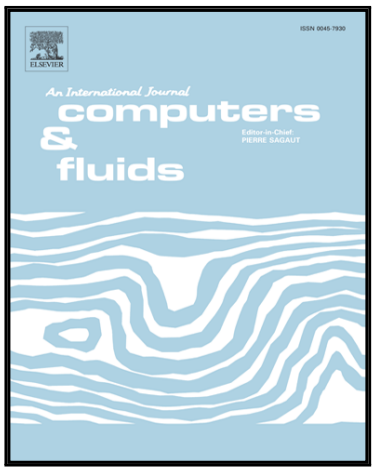

Modelling biological and bio-inspired swimming at microscopic scales: recent results and perspectives

Giancarlo Cicconofri, Antonio DeSimone

PII: S0045-7930(18)30424-9
DOI: https://doi.org/10.1016/j.compfluid.2018.07.020
Reference: CAF 3962

To appear in: *Computers and Fluids*

Received date: 11 December 2017
Revised date: 9 July 2018
Accepted date: 31 July 2018

Please cite this article as: Giancarlo Cicconofri, Antonio DeSimone, Modelling biological and bio-inspired swimming at microscopic scales: recent results and perspectives, *Computers and Fluids* (2018), doi: https://doi.org/10.1016/j.compfluid.2018.07.020

This is a PDF file of an unedited manuscript that has been accepted for publication. As a service to our customers we are providing this early version of the manuscript. The manuscript will undergo copyediting, typesetting, and review of the resulting proof before it is published in its final form. Please note that during the production process errors may be discovered which could affect the content, and all legal disclaimers that apply to the journal pertain.

ACCEPTED MANUSCRIPT

Highlights

- conceptual principles behind control and steering of swimming micro-organisms
- periodic beating of flagella leads to helical trajectories (helix theorem)
- coupling of body rotations with helical motion explains phototactic guidance
- the validity of the helix theorem is extended to ciliated micro-organisms
- a principle for self-assembly explains why helices are so recurrent in nature

ACCEPTED MANUSCRIPT

ACCEPTED MANUSCRIPT

Modelling biological and bio-inspired swimming at microscopic scales: recent results and perspectives

Giancarlo Cicconofri[a], Antonio DeSimone[b,*]

[a] *GSSI - Gran Sasso Science Institute, viale Francesco Crispi 7, 67100 L'Aquila - Italy*
[b] *SISSA - International School for Advanced Studies, via Bonomea 265, 34136 Trieste - Italy*

Abstract

Some recent results on biological and bio-inspired swimming at microscopic scales are reviewed, and used to identify promising research directions for the future. We focus on broad conceptual principles such as looping in the space of shapes, loss of controllability of systems in which shape is only partially controlled, and steering by modulating the actuation rate. Moreover, we discuss propulsion mechanism that are most common for unicellular swimmers, such as flagellar and ciliary beating, and we examine amoeboid motion and flagellar propulsion in Euglena. The Helix Theorem, a universal law characterising orbits traced by ciliated and flagellated unicellular swimmers propelled by the periodic beating of cilia and flagella, is proved and discussed as a principle of self-assembly for helical structures.

Keywords: low Reynolds number flows, micro-swimmers, helical trajectories, fluid-structure interaction, control of Stokes system, cell motility, soft robotics

1. Introduction

Cells are the fundamental units of life, and many of the processes responsible for the functioning and fate of living organisms are governed by biological machines. For example, the response of the immune system to a wound is organised through the recruitment of leukocytes from blood vessels, and their migration to the site of the wound, where they attack and dispose of pathogenic intruders. Many coordinated processes are needed for the correct functioning of this complex response, but cell motility, namely, the capability of certain unicellular organisms (the leukocytes) to reach a target position (the site of the wound) and then chase pathogens is clearly crucial. This example can be vastly generalised to many other biological functions: the successful swimming of a single sperm cell to its target egg cell, for example, is at the origin of (almost) every human being. The study of cell motility is therefore an important chapter of biology. And, quoting Cohen (2004), mathematics is biology's next microscope, only better.

Interestingly, our bodies host a large number of unicellular organisms (including, for example, bacteria) that are capable of moving around it quite freely and proficiently. Yet, we are still unable to engineer systems of microscopic size capable of reproducing at least some of the abilities of these exquisite biological machines. Not surprisingly, interest is growing on the possibility of manufacturing micro-machines that could perform some useful function within a human body, such as imaging, or delivering drugs to specific locations, or performing small surgeries such as

*Corresponding author.
Email address: desimone@sissa.it (Antonio DeSimone)

ACCEPTED MANUSCRIPT

ACCEPTED MANUSCRIPT

removing material or patching small wounds Ornes (2017). Quoting Feynman (1960), it would be interesting in surgery if you could swallow your surgeon.

Motivated by this challenging and exciting background, in the last few years we have been involved in conducting research on the mathematical modelling of cell motility. As a part of this effort, we have studied locomotion based on the interactions between a cell and a surrounding fluid, namely, swimming of unicellular organism. The field has been blessed by the attention of some scientific giants (Taylor (1951); Purcell (1977); Shapere and Wilczeck (1989)), and is enjoying considerable attention in the current research literature. Excellent recent reviews are available, e.g., Lauga and Powers (2009); Gaffney et al. (2011); Guasto et al. (2012); Goldstein (2015). Together with the papers cited therein they provide the interested reader with several hundred references to explore the state-of-the-art.

In this paper, we review some of our recent results on biological and bio-inspired swimming at microscopic scales, and use them to look ahead at promising research directions for the future. Our emphasis will be on conceptual principles of general validity, that can help rationalise the observed behaviour of complex biological organisms. The idea is to use mathematical modelling as the tool to extract some templates, which yield the "secrets" of their successful performance. Bio-inspiration has a great and rather unexplored potential at this level of abstraction, and we see in this field an opportunity for mathematical biology to contribute and help to go beyond the more traditional approaches of bio-mimetics and bio-mimicry.

The lessons learned from the study of biological organisms can inform the design of new bio-inspired engineered devices. Conversely, looking back at biology through the functionalist view of an engineer wishing to replicate its successes can help us to understand how biological machines function, with a level of detail which is unprecedented.

The rest of the paper is organised as follows. Section 2 describes the mathematical formulation of the swimming problem, setting the stage for our discussion. We illustrate in Section 3 some key conceptual principles of swimming motility at microscopic scales such as: looping in the space of shapes; the distinction between swimming with prescribed shapes and cases where shape is partly controlled and partly emergent from the competition of hydrodynamic resistance and elastic restoring forces; the loss of controllability in the second scenario; and steering by modulation of the rate of actuation. In Section 4 we review the most common mechanisms used by unicellular swimmers, which are based on the beating of flexible cilia and flagella, and we continue in Section 5 with an in-depth case-study of Euglena gracilis. This protist exhibits two very different forms of motility, namely, amoeboid motion or metaboly and swimming by flagellar propulsion. The latter leads us to discuss the Helix Theorem, a universal law for the orbits traced by micro-organisms that swim in free-space under the propulsive action of a periodically beating system of flagella or cilia. The same theorem, interpreted as principle for self-assembly of helical structures, is used to explain their ubiquity in nature.

Finally, in Section 6, we argue that the growing need for the accurate evaluation of the details of the flows induced by unicellular organisms, or of reliable tools and algorithms for motion planning and control of bio-inspired micro-robots represents an opportunity for the future development of new numerical tools for the solution of fluid-structure interaction and control problems.

2. Swimming at low Reynolds numbers: mathematical model

We describe the motion of a generic swimmer through a (time-dependent) shape map $t \mapsto \bar{\Phi}_t$, which specifies the way the reference configuration $\mathcal{B}$ changes in time as seen from a reference frame moving with the swimmer (body-frame), and through the way the body frame evolves with respect to the lab-frame. The current position and orientation of the body-frame are given

ACCEPTED MANUSCRIPT

Figure 1: Reference and deformed configurations of the swimmer: parametrisation in terms of positional and orientational change, and shape change.

by the position of the origin, $\mathbf{c}(t)$, while the axes are obtained from the axes of the lab-frame through the rotation $\mathbf{R}(t)$. In formulas (see also Figure 1),

$$\Phi_t(X) = \mathbf{c}(t) + \mathbf{R}(t)\bar{\Phi}_t(X) = (\mathbf{c}(t) + \mathbf{R}(t)id(X)) + \mathbf{R}(t)\bar{\mathbf{u}}_t(X) \tag{1}$$

where, in the second identity, we have written $\bar{\Phi}_t$ as the sum of the identity map id plus a displacement $\bar{\mathbf{u}}_t$. This emphasizes that $\Phi_t(X)$ consists of a rigid motion (the one in brackets), and of a genuine change of shape associated with $\bar{\mathbf{u}}_t$.

The map (1) gives the position x at time t of a (material) point $X \in \mathcal{B}$ of the swimmer. Given a point $x \in \mathcal{B}_t = \Phi_t(\mathcal{B})$, this is the position at time t of the point

$$X = \Phi_t^{-1}(x) = \bar{\Phi}_t^{-1}(\mathbf{R}^T(t)(x - \mathbf{c}(t))) \tag{2}$$

The (Lagrangian) velocity of a (material) point of the swimmer is the time derivative of (1),

$$\dot{\Phi}_t(X) = \dot{\mathbf{c}}(t) + \dot{\mathbf{R}}(t)\bar{\Phi}_t(X) + \mathbf{R}(t)\dot{\bar{\Phi}}_t(X) \tag{3}$$

where superposed dots denote time derivatives. The (Eulerian) velocity of the point of the swimmer occupying place x at time t is

$$\dot{\Phi}_t\left(\Phi_t^{-1}(x)\right) = \dot{\mathbf{c}}(t) + \omega(t) \times (x - \mathbf{c}(t)) + \mathbf{R}(t)\dot{\bar{\Phi}}_t\left(\bar{\Phi}_t^{-1}\left(\mathbf{R}^T(t)(x - \mathbf{c}(t))\right)\right) \tag{4}$$

where $\omega(t)$ is the axial vector associated with the skew-symmetric matrix $\dot{\mathbf{R}}(t)\mathbf{R}^T(t)$.

Shape changes of the swimmer induce motion of the surrounding fluid. Dealing with microscopic scales (so that the Reynolds number is small) and assuming that the rate at which shape changes occur are not exceedingly fast (so that the Womersley number is also small), we model the flow with the stationary Stokes system, so that the velocity $\mathbf{u}$ and pressure p in the fluid satisfy

$$\eta\Delta\mathbf{u} - \nabla p = 0 \quad \text{and} \quad \operatorname{div}\mathbf{u} = 0 \quad \text{in } \mathbb{R}^3 \setminus \mathcal{B}_t \tag{5}$$

where η is the viscosity of the fluid, together with the no-slip condition at the interface between the fluid and the swimmer boundary

$$\mathbf{u}(x,t)|_{\partial\mathcal{B}_t} = \dot{\Phi}_t\left(\Phi_t^{-1}(x)\right)|_{\partial\mathcal{B}_t} \tag{6}$$

and suitable decay conditions at infinity. This outer Stokes problem is well posed, and given the one-parameter family of Dirichlet data $t \mapsto \mathbf{u}(x,t)|_{\partial\mathcal{B}_t}$ (i.e., given the maps $t \mapsto \mathbf{c}(t), \mathbf{R}(t), \bar{\Phi}_t$), the velocity $\mathbf{u}(x,t)$ and pressure $p(x,t)$ distributions in the fluid are uniquely determined.

ACCEPTED MANUSCRIPT

The motion of the swimmer is governed by the balance of linear and angular momentum. We neglect inertia, and all other external forces different from those exerted by the fluid. So the balance of linear and angular momentum become the statement that the total force and torque exerted on the swimmer by the surrounding fluid vanish. Denoting the Cauchy stress in the fluid with

$$\mathbf{S}[\mathbf{u}](x,t) = -p(x,t)\mathbf{Id} + \eta\left(\nabla\mathbf{u}(x,t) + \nabla\mathbf{u}^T(x,t)\right) \tag{7}$$

we write these as

$$0 = \mathbf{f}(t) = \int_{\partial\mathcal{B}_t} \mathbf{S}[\mathbf{u}](x,t)\mathbf{n}(x)\mathrm{dA} \quad \text{and} \quad 0 = \mathbf{g}(\mathrm{t}) = \int_{\partial\mathcal{B}_t} (\mathrm{x} - \mathbf{c}(\mathrm{t}) \times \mathbf{S}[\mathbf{u}](\mathrm{x},\mathrm{t})\mathbf{n}(\mathrm{x})\mathrm{dA} \tag{8}$$

where $\mathbf{n}(x)$ is the outer unit normal at $x \in \partial\mathcal{B}_t$. It turns out that, given $t \mapsto \bar{\Phi}_t$, equations (8) determine uniquely the two time-dependent vectors $\bar{\mathbf{v}}(t) = \mathbf{R}^T(t)\dot{\mathbf{c}}(t)$ and $\bar{\omega}(t) = \mathbf{R}^T(t)\omega(t)$, namely, the representations in the body-frame of $\dot{\mathbf{c}}(t)$ and $\omega(t)$. Thus, $\mathbf{c}(t)$ and $\mathbf{R}(t)$ are found by integrating the equations $\dot{\mathbf{c}}(t) = \mathbf{R}(t)\bar{\mathbf{v}}(t)$ and $\dot{\mathbf{R}}(t) = \mathbf{R}(t)[\bar{\omega}(t)]_\times$ (where the skew-symmetric tensor $[\bar{\omega}(t)]_\times$ is defined by $[\bar{\omega}(t)]_\times\mathbf{a} = \bar{\omega}(t) \times \mathbf{a}$ holding for every vector $\mathbf{a}$). This shows that the following

Swimming Problem: given a history of swimmer shapes $t \mapsto \bar{\Phi}_t$, find the corresponding history of positions and orientations $t \mapsto \mathbf{c}(t), \mathbf{R}(t)$

has a unique solution. This is proved in full detail in Dal Maso et al. (2011).

A further interesting question is whether, given initial position and orientation $\mathbf{c}(0), \mathbf{R}(0)$ and a target position $\mathbf{c}(0) + \Delta\mathbf{c}$ (or a target position and orientation pair), there exist a shape history $t \mapsto \bar{\Phi}_t$ such that the swimmer can reach the target. This is a typical question of control theory. In fact, swimming is a perfect example of exploiting fluid-structure interactions to control the (Navier)-Stokes equations: we use shape changes and act on the fluid to produce flows that generate exactly those forces that propel the swimmer in the desired way.

3. Locomotion principles

In this section, we use the framework introduced in Section 2 to discuss some general locomotion principles. We do this by focusing on some simple, yet representative examples.

3.1. No looping? No party!

A simple system which is of great conceptual value is the three-sphere-swimmer proposed in Najafi and Golestanian (2004). Consider the case in which $\mathcal{B}$ consists of three rigid spheres of equal radius, whose centres are aligned and constrained to move along one line parallel to the unit vector $\mathbf{e}$, only varying their mutual distances $L + \bar{u}_1(t), L + \bar{u}_2(t)$ (see Figure 2). The position of every point of the system is specified, once we know the positions of the three centres

$$x_1(t) = c(t) - (L + \bar{u}_1(t))\,, \quad c(t)\,, \quad x_2(t) = c(t) + (L + \bar{u}_2(t))\,. \tag{9}$$

We will only follow these while considering a T-periodic shape change

$$t \mapsto \bar{\mathbf{u}}(t) = (\bar{u}_1(t), \bar{u}_2(t)) \tag{10}$$

a closed curve in the space of shapes, which for concreteness we will assume to be traced in the anti-clockwise direction.

ACCEPTED MANUSCRIPT

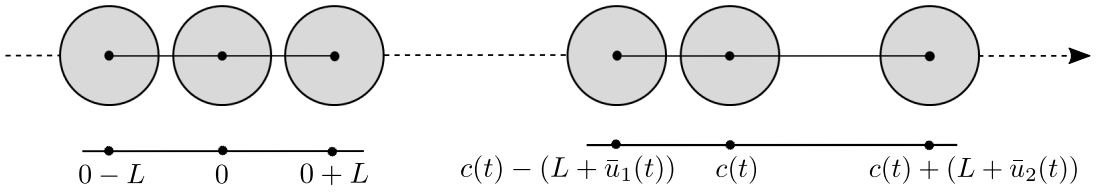

Figure 2: Three-sphere-swimmer: parametrisation in terms of positional change, and shape change.

Linearity of the Stokes system leads to linear dependence of the forces in (8) on the Dirichlet data of the outer Stokes problem, hence on $\dot{c}, \dot{\bar{u}}_1, \dot{\bar{u}}_2$. The component along $\mathbf{e}$ of the force balance is then written as

$$0 = f(t) = f_1(\bar{\mathbf{u}}(t))\dot{\bar{u}}_1(t) + f_2(\bar{\mathbf{u}}(t))\dot{\bar{u}}_2(t) + f_3(\bar{\mathbf{u}}(t))\dot{c}(t) \tag{11}$$

where, in view of translational invariance, the force coefficients are independent of position and depend only on shape. Solving for $\dot{c}$ we obtain

$$\dot{c}(t) = \mathbf{V}(\bar{\mathbf{u}}(t)) \cdot \dot{\bar{\mathbf{u}}}(t)\,, \quad \text{where} \quad V_i(\bar{\mathbf{u}}(t)) := -\frac{f_i(\bar{\mathbf{u}}(t))}{f_3(\bar{\mathbf{u}}(t))} \tag{12}$$

Using Stokes theorem, we obtain the displacement Δc in one stroke as

$$\Delta c = \int_0^T \mathbf{V}(\bar{\mathbf{u}}(t)) \cdot \dot{\bar{\mathbf{u}}}(t) dt = \int_\omega \mathrm{curl}_{\bar{\mathbf{u}}} \mathbf{V}(\mathrm{u}_1, \mathrm{u}_2) \mathrm{d}\mathrm{u}_1 \mathrm{d}\mathrm{u}_2 \tag{13}$$

where $\mathrm{curl}_{\bar{\mathbf{u}}} \mathbf{V} = \partial \mathrm{V}_2/\partial \bar{\mathrm{u}}_1 - \partial \mathrm{V}_1/\partial \bar{\mathrm{u}}_2$ and ω is the region of shape space enclosed by the closed curve (10).

As emphasised in Alouges et al. (2008), formula (13) above summarises several cornerstone results of low Reynolds number swimming. The first one is that, if the closed curve $\partial\omega$ spans zero area (i.e., the loop in shape space is trivial, as it happens for a reciprocal shape change), then the displacement vanish. This is the so-called *Scallop Theorem* of Purcell (1977), stating that, without inertia, a scallop-like organism that can only open and close its valves cannot swim.

The second important result is that, even when the loop in shape space is non-trivial, the displacement is zero if the integrand in (13) vanishes. Therefore, swimming rests on the fact that *hydrodynamic resistance forces* (the f_i's defining the vector field $\mathbf{V}$ in (12)) *are shape-dependent*, as probed by the differential operator $\mathrm{curl}_{\bar{\mathbf{u}}}$.

The third fact following from (13) is that the displacement in one stroke is *geometric*: it only depends on the geometry of the loop drawn in the space of shapes, (10), not on the speed at which the loop is traced.

Finally, formula (13) shows that the system is fully *controllable*. Indeed, if $\Delta c \neq 0$ is the displacement achieved with the loop Γ, smaller displacements of the same sign can be achieved with loops of smaller area, any positive multiple $k\Delta c$ can be achieved by tracing Γ k times, and $-\Delta c$ can be obtained by tracing Γ in the opposite direction.

3.2. Minimal swimmers with or without directional control

Building on the results of the previous section, we want to ask now the question: What is the minimal number of independent motors, or controllers, that can allow the three-sphere swimmer

ACCEPTED MANUSCRIPT

to achieve non-zero net displacements? A superficial answer would be: two. However, as shown in Montino and DeSimone (2015), the correct (and, at first sight, surprising) answer is: one.

Indeed, by replacing one of the "arms" between two consecutive spheres with a passive spring, and actuating periodically the remaining one, once can still extract net displacements, because the two arm lengths can still describe a loop in the space of shapes. To understand how this arises, consider the two limit cases of very slow and very fast actuation frequencies. At low actuation frequencies, the viscous forces are negligible with respect to the elastic ones, and the system behaves as if it had one rigid arm (hence, no net displacements). At high actuation frequencies, elastic forces are negligible with respect to viscous ones, and the system behaves as a collection of three beads, one of which is free, while the distance between the other two is oscillating. It is relatively straightforward to show that, in this case, long range hydrodynamic interactions lead to synchronisation of the three spheres, and the two distances (the arm lengths) oscillate keeping their sum constant. At intermediate actuation frequency ω, elastic and viscous forces compete, and the dynamics of the system leads to the two distances oscillating at the same frequency, but with a frequency-dependent (locked) phase difference which is controlled by the non-dimensional parameter

$$\Omega := \frac{\omega \eta L}{K} \,. \tag{14}$$

Here K is the stiffness of the passive spring, L its rest length, and η is the fluid viscosity. Thanks to this phase lag, the two arm lengths trace a non-trivial loop in the space of shapes, leading to non-zero (frequency dependent) net displacements in one cycle.

The gain in simplicity associated with getting rid of independent control of one the two arms comes, however, with a cost in terms of the performance of the device. This is the loss of controllability. Indeed, since the phase lag is set by system properties that cannot be tuned, see (14), the loops in the space of shapes will be traced with a fixed phase lag, hence in a fixed direction. The sign of the displacement is then hard-wired into the system and the three-sphere swimmer with one passive arm can only move with the passive arm ahead, see Montino and DeSimone (2015). Put differently, one motor/controller leads to the minimal system capable of achieving non-zero net displacements, but without a reverse gear. Two independent motors/controllers are necessary for a controllable system.

3.3. Steering by modulation of the actuation speed

In Cicconofri and DeSimone (2016) we studied a low Reynods number swimmer that reveals some surprising features when contrasted with the observations in Section 3.1. The swimmer consists of a (rigid) spherical head with an elastic tail attached to it, as schematically depicted in Figure 3. We considered planar motions of the system, assuming that the swimmer can actively control only the angle α between the head and the tail. We studied the resulting swimming motion under generic periodic time histories $t \to \alpha(t)$ of the control parameter, resulting in periodic tail beating.

The first surprising feature of the system is the ability of the swimmer to propel itself and to "steer", following either straight or curved trajectories (on average, after many beats), despite being actuated by only *one* control parameter. Secondly, the resulting displacements after each beating period are not geometric: Changing the speed of the periodic control α *does* change the resulting displacement. There is no contradiction, however, between these results and the observations in Section 3.1. The key to realise this is that, in the swimmer of Figure 3, shape is not completely prescribed, because of the presence of the elastic tail. The shape of the latter is not *a-priori* known, and it only *emerges* from the balance of elastic and hydrodynamic forces arising from the actuation of the angle α. Thus, moving from systems in which shape is completely

ACCEPTED MANUSCRIPT

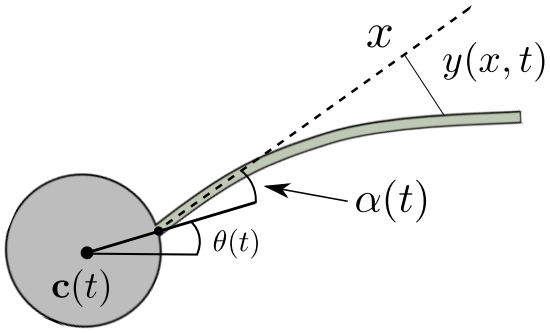

Figure 3: Swimmer with elastic tail. The moving frame of the swimmer is given by the centre $\mathbf{c}$ and the orientation θ of the head. The swimmer controls the angle α between its spherical head and its tail at the point of attachment.

controlled to systems in which shape is partly emergent, the picture changes completely with respect to the Scallop Theorem scenario of Purcell (1977).

We considered the equations of motion of the system in the local drag approximation of Resistive Force Theory, see Lauga and Powers (2009), restricting our analysis to stiff-tailed swimmers. This allowed us to obtain analytical results in the small parameter regime $\epsilon \ll 1$ where ϵ is the ratio between the typical viscous and elastic force acting on the tail. A formula that sheds light on the behaviour of the system during its motion is the one proved in Cicconofri and DeSimone (2016) for the (normalized) deviation $y(x,t)$ of the tail from its straight configuration

$$y(x,t) = -\epsilon p(\alpha(t), x)\dot{\alpha}(t) + \mathcal{O}(\epsilon^2)\,, \tag{15}$$

see Figure 3. The function $p(\alpha, x)$ in equation (15), which can be calculated explicitly, is a positive polynomial with α-dependent coefficients in the variable x. The dependence of the deviation y on the velocity $\dot{\alpha}$ of the angle α has a simple physical reason: The faster the tail beats, the larger are the viscous forces acting on it, which result in larger bending of the tail itself. The critical consequence of (15) follows from another simple observation: given the position of centre $\mathbf{c}$ and the orientation θ of the swimmer's head (see Figure 3), the configuration of the swimmer is fully determined by the angle α and the deviation y. That is, α and y determine the shape of the swimmer. What (15) shows, then, is that the shape of the swimmer in motion is fully determined (at least at first approximation) by the angle α and its rate-of-change $\dot{\alpha}$, which, in turn, can be considered as a shape parameter.

Indeed, a loop in the shape-space of the elastic tail swimmer can be effectively given by the closed curve $t \to (\alpha(t), \dot{\alpha}(t))$. Consistently with the basic principles stated in Section 3.1, we showed that net displacements $\Delta\mathbf{c}$ and net rotations $\Delta\theta$ of the swimmer arise because of this looping. More precisely, denoting ω the two dimensional set enclosed by the loop $t \to (\alpha(t), \dot{\alpha}(t))$, we derived the following formulas

$$\Delta\mathbf{c} = \epsilon \int_\omega \mathbf{U}(\alpha,\psi)d\alpha d\psi + \mathcal{O}(\epsilon^2) \quad \text{and} \quad \Delta\theta = \epsilon \int_\omega W(\alpha,\psi)d\alpha d\psi + \mathcal{O}(\epsilon^2)\,, \tag{16}$$

where $\mathbf{U}$ and W are two non-vanishing functions (vector-valued and scalar-valued, respectively) which are independent on the loop itself. At leading order in ϵ, formulas (16) have the exact same structure of equation (13).

From (16) we can derive the characteristic motion control capabilities of the swimmer. First, we can conclude that propulsion is possible, since a loop $t \to (\alpha(t), \dot{\alpha}(t))$ naturally spans non-zero

ACCEPTED MANUSCRIPT

area, as one can see in the simple case $\alpha(t) = \sin t$. Second, (16) explains why displacements are non-geometrical. For example, a simple time rescaling $t \to \lambda t$ results in a deformation of the shape parameters loop $t \mapsto (\alpha(\lambda t), \lambda\dot{\alpha}(\lambda t))$, thus faster (or slower) beating results in different displacements. More general modulations of the velocity of beating can be considered, resulting in different geometries of the shape parameters loop. This gives room for motion control, so the swimmer can couple displacements and rotation during each period (steering). It is possible to show that the swimmer follows curved trajectories in the case of asymmetric beating, when α undergoes a fast up-beat followed by a slow down-beat during one period.

4. How do biological micro-swimmers swim?

It may seem surprising that the principles discussed above may have anything to teach us about the locomotion strategies of unicellular organisms, which look very different from the systems of beads and springs analysed in Section 3. In fact, this is indeed the case, as we argue in the remainder of this section by showing that the principle discussed in Section 3.1 goes a long way in rationalising observed behaviour in Biology.

4.1. Chlamydomonas' breaststroke

Chlamydomonas is a unicellular alga, with a round body, which swims thanks to the beating of two flexible anterior flagella, see e.g. Guasto et al. (2010); Goldstein (2015). It has been used as a model organism, in particular for what concerns flagellar locomotion Drescher et al. (2010).

In one of its typical behaviours, the cell beats the two flagella in synchrony in a plane, symmetrically about a central symmetry axis of the body. With this perfect breast-stroke, the cell progresses with a rocking back-and-forth motion along the symmetry axis. Net displacements are made possible by the fact that the shape of the flagella varies during one stroke cycle. They are extended during the power phase of the stroke, when the flagella beat (say) downwards, and push the cell body upwards. They are contracted in the recovery part of the stroke, when they move upwards to recover the initial posture, and push the cell downwards (hence the rocking motion). Net upward displacement results from the fact that the hydrodynamic forces generated by the extended flagellum are higher than those generated by the retracted flagellum, moving in the opposite direction. Considering as shape variables the angle formed at the attachment of the body (localised curvature), and a measure of global curvature, we see that Chlamydomonas' breast stroke consists of a loop in the space of shapes.

This mechanism is ubiquitous also in the self-propulsion of ciliates, which are typically covered by numerous arrays of beating cilia. Their beating is typically organised in periodic spatio-temporal patterns called metachronal waves. Individual cilia oscillate back and forth with a shape asymmetry between an extended configuration in the power phase and a more bent one during recovery.

4.2. Sperm cells, flagellar beating, and travelling waves

Sperm cells are among the most thoroughly studied examples of unicellular swimmers, see e.g. Gaffney et al. (2011). There is hardly a more evident illustration of how cell motility is relevant to life as the (swimming) event that is common to every human being (or, at least, to the overwhelming majority of them). Namely, that of a sperm cell that successfully swims its way until it reaches and fecundates an egg cell.

Sperm cells move by beating a flagellum, whose structure is highly conserved across eukaryotic species. It consists of longitudinal bundles of microtubules, arranged in a precise spatial structure, on which molecular motors exert forces that cause the creation and propagation of longitudinal

ACCEPTED MANUSCRIPT

bending waves. These bending waves generate the propulsive forces powering the motion of the cell.

A travelling wave of bending is therefore a very common shape change propelling a large number of unicellular swimmers, and the mechanism by which it produces propulsion was analysed in the seminal paper Taylor (1951), one of the milestones of the whole literature on biological fluid dynamics at microscopic scales. The traveling waves of bending studied in this paper are of the form

$$\bar{u}(X,t) = b\sin(kX - \omega t) = b\cos(\omega t)\sin(kX) - b\sin(\omega t)\cos(kX)\,, \tag{17}$$

which shows how they represent a loop (in fact, a circle, since $\cos^2(\omega t) + \sin^2(\omega t) = 1$) in a space of shapes parametrised by the two wave forms $\sin(kX)$ and $\cos(kX)$.

5. A case study: Euglena gracilis

We have been studying Euglenids, see Leander et al. (2017), and Euglena gracilis in particular already for a few years. The reason of our interest in this protist, a unicellular flagellate, is that it exhibits two distinct forms of motility. One is through the beating of a single anterior flagellum (swimming motility). Another one is through very large, elegantly coordinated, rhytmic shape changes of the whole body (amoeboid motion or metaboly). What controls the switching between this two distinct "gaits" is an interesting question, which is still open, and on which we have some hypotheses.

5.1. Metaboly and mechanisms for shape change

The large shape changes associated with metaboly correlate closely with geometric rearrangements of the pellicle structure underneath the plasma membrane. This is a complex made of protinaceous pellicle strips, microtubules, and molecular motors. The strips have overlap regions and are able to slide one on another along their length. The sliding is powered by molecular motors that induce sliding in the microtubules that run parallel to the strips, along the overlap region. The relative sliding along the strips can be thought of as a mechanism of active surface shearing or, in the language of differential geometry, of active change in the surface metric. In view of Gauss' Theorema Egregium, modulating the pellicle shears means modulating the surface metric along the surface, and this can produce (Gaussian) curvature.

Interestingly, the propulsive mechanism associated with metaboly consists of the propagation of a round protruding bulge along the axis of an elongated body of approximately cylindrical shape. A surface with a bulge is one with nonzero Gaussian curvature, so that metaboly relies on the propagation of nonzero Gaussian curvature along the cell body. This can be accomplished and, as experiments show, is in fact accomplished by modulation of the pellicle shears along their lengths. And in the regions where the bulge forms, the pellicle strips acquire a characteristic helical shape. This mechanism is described in detail in Arroyo et al. (2012); Arroyo and DeSimone (2014).

Further details on metaboly as a form of motility, and on the mechanisms controlling how Euglena switches to this mode of behaviour are discussed in Noselli et al. (2018).

5.2. Helical trajectories and a principle for self-assembly

In Rossi et al. (2017), we have recently managed to reconstruct the three-dimensional trajectories and flagellar shapes of swimming Euglena, starting from time-sequences of two-dimensional images obtained with an optical microscope. This has been made possible thanks to the precise characterisation of the orbits (the maps $t \mapsto \mathbf{c}(t), \mathbf{R}(t)$ of the swimming problem of Section 2)

ACCEPTED MANUSCRIPT

traced by an object propelled by a flagellum beating periodically in time. Hydrodynamics of Stokes flows (the one commonly used for micro-swimmers) dictates the following *universal law of periodic flagellar (and ciliar) propulsion*: the orbits of any object propelled by periodically beating flagella (or cilia), swimming far away from walls, boundaries, etc. are always generalised helices. This makes the reconstruction of three-dimensional trajectories possible: once the three-dimensional geometric structure of the orbits is known, these can be obtained from their two-dimensional projections, hence *lifting* the two-dimensional experimental images to three dimensions.

In fact, the same result on helical trajectories holds true if the organism is propelled by an array of cilia, beating periodically. This situation is typically modelled treating the swimmer as a *squirmer*, i.e. a rigid body with a distribution of slip velocities on its boundary, which represent the relative velocity of the fluid (which moves like the tips of the cilia) with respect to the base of the cilia, attached to the boundary of the body. If the slip velocity field is periodic in time, the resulting orbits are generalised helices. For the sake of simplicity, we will illustrate the results on helical swimming above by only considering the discrete curve traced by an arbitrary point of the swimmer (the origin $\mathbf{c}(t)$ of the body-frame), following its positions after integer multiples of the beating period T. We have the following:

Helix Theorem The discrete trajectory $k \mapsto \mathbf{c}_k = \mathbf{c}(0+kT)$ traced by a micro-swimmer moving in free-space, propelled by the T-periodic beating of a flagellum or of an array of cilia, is a discrete circular helix.

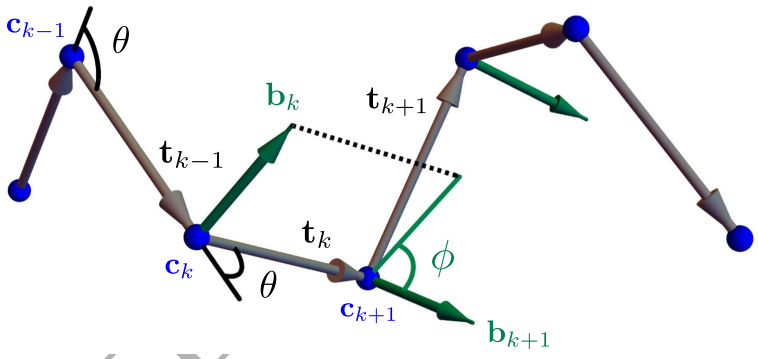

Figure 4: Tangents and binormals to the discrete helix to compute curvature $\theta/|\mathbf{d}|$ and torsion $\phi/|\mathbf{d}|$.

While this result is a special case of a more general one proved in Rossi et al. (2017), we give in the following a (new) direct proof. Assume that, at $t = 0$, body-frame and lab-frame coincide: $\mathbf{c}(0) = \mathbf{o}$, $\mathbf{R}(0) = \mathbf{Id}$, and let $\mathbf{d}$ and $\mathbf{R}$ be the displacement and rotation at the end of one beat cycle. After each cycle, the incremental displacement and rotation *in the body-frame* will always be $\mathbf{d}$ and $\mathbf{R}$ since the shape change cycle is the same, and the swimming problem (written in the body-frame) is invariant by rotation and translation. Composing these (constant) translations and rotations with the motion of the body-frame, the discrete trajectory in the lab-frame will be

$$\mathbf{c}_k = \mathbf{o} + \mathbf{d} + \mathbf{R}\mathbf{d} + \mathbf{R}^2\mathbf{d} + \ldots + \mathbf{R}^{(k-1)}\mathbf{d}\,, \quad \text{and} \quad \mathbf{R}_k = \mathbf{R}^k\,, \tag{18}$$

where $\mathbf{R}_k = \mathbf{R}(0 + kT)$ and $\mathbf{R}^0 = \mathbf{R}(0) = \mathbf{Id}$.

To see that $(18)_1$ is a discrete circular helix, we will use the discrete version of a result form differential geometry, usually attributed to Lancret: a curve with constant curvature and torsion

is necessarily a circular helix. To compute the (discrete) curvature at point $\mathbf{c}_k$, consider the (osculatory) plane generated by the three points $(\mathbf{c}_{k-1}, \mathbf{c}_k, \mathbf{c}_{k+1})$ and spanned by the (discrete) tangents $\mathbf{R}^{(k-1)}\mathbf{d}$ and $\mathbf{R}^{(k-1)}\mathbf{R}\mathbf{d}$, see Figure 4. By Frenet's formulas, the curvature at $\mathbf{c}_k$ is $1/|\mathbf{d}|$ times the angle θ between $\mathbf{d}$ and $\mathbf{R}\mathbf{d}$, which is independent of k. Similarly, to compute the torsion at point $\mathbf{c}_k$, consider the binormal at $\mathbf{c}_k$. This is orthogonal to the osculatory plane at $\mathbf{c}_k$, hence parallel to $\mathbf{R}^{(k-1)}(\mathbf{d} \times \mathbf{R}\mathbf{d})$. Similarly, the binormal at $\mathbf{c}_{k+1}$ is orthogonal to the plane spanned by $\mathbf{R}^k\mathbf{d}$ and $\mathbf{R}^{(k+1)}\mathbf{d}$, hence parallel to $\mathbf{R}^{(k-1)}(\mathbf{R}(\mathbf{d} \times \mathbf{R}\mathbf{d}))$. By Frenet's formulas, the torsion at $\mathbf{c}_k$ is $1/|\mathbf{d}|$ times the angle ϕ between $\mathbf{d} \times \mathbf{R}\mathbf{d}$ and $\mathbf{R}(\mathbf{d} \times \mathbf{R}\mathbf{d})$, which is independent of k. Special cases are that of a straight trajectory, which arises when $\mathbf{d}$ is parallel to the axis of $\mathbf{R}$ (hence $\mathbf{d} \times \mathbf{R}\mathbf{d} = 0$, zero discrete curvature), and of a circular trajectory, which arises when $\mathbf{d}$ is perpendicular to the axis of $\mathbf{R}$ (so that both $\mathbf{d} \times \mathbf{R}\mathbf{d}$ and $\mathbf{R} \times (\mathbf{d} \times \mathbf{R}\mathbf{d})$ are parallel to the axis of $\mathbf{R}$ and hence, zero discrete torsion).

The (informal) discussion above can be made rigorous by using the results in Carroll et al. (2014), that show that curve $(18)_1$ can be seen as the discretisation of a continuous curve having as curvature and torsion exactly the values computed from $(18)_1$.

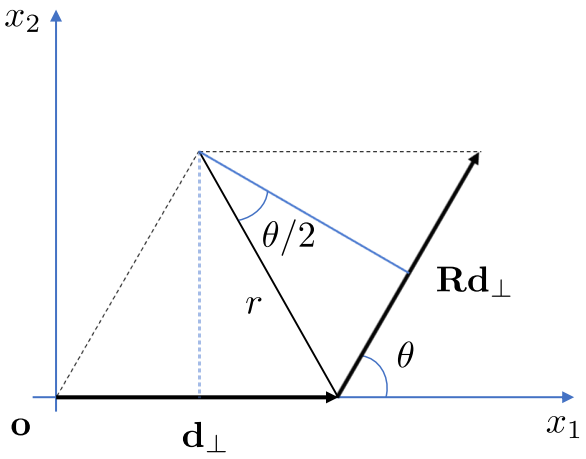

Figure 5: Geometric construction of the parameters of the discrete circular helix associated with shift $\mathbf{d}$ and rotation $\mathbf{R} = \mathbf{R}^\theta_\mathbf{e}$ of angle θ and axis $\mathbf{e}$. In the figure, $\mathbf{d}_\perp$ denotes the projection of $\mathbf{d}$ on the plane perpendicular to the rotation axis $\mathbf{e}$.

It is interesting to give a concrete geometric representation of the helix above, see Figure 5. Let $\mathbf{e}$ be the axis of the rotation $\mathbf{R}$ (the eigenvector corresponding to its eigenvalue equal to $+1$) and θ the angle. We can highlight the two parameters characterising the rotation $\mathbf{R}$ by writing $\mathbf{R} = \mathbf{R}^\theta_\mathbf{e}$. In a reference frame with origin $\mathbf{o}$, first axis aligned with $\mathbf{d}_\perp$, the projection of $\mathbf{d}$ on the plane perpendicular to the rotation axis $\mathbf{e}$ (we are assuming here that $\mathbf{d}$ is not parallel to $\mathbf{e}$, for otherwise the trajectory is a straight line parallel to $\mathbf{d}$), and third axis aligned with $\mathbf{e}$, the equation of the discrete circular helix $(18)_1$ is

$$x_1(k) = r\cos\left(\frac{\pi-\theta}{2}\right) + r\cos\left(-\frac{\pi+\theta}{2} + k\theta\right) \tag{19}$$

$$x_2(k) = r\sin\left(\frac{\pi-\theta}{2}\right) + r\sin\left(-\frac{\pi+\theta}{2} + k\theta\right) \tag{20}$$

ACCEPTED MANUSCRIPT

$$x_3(k) = 0 + k\,|\mathbf{d}_{//}| \tag{21}$$

where

$$r = \frac{|\mathbf{d}_\perp|/2}{\sin(\theta/2)}\,, \quad \mathbf{d}_{//} = (\mathbf{e}\otimes\mathbf{e})\,\mathbf{d}\,, \quad \mathbf{d}_\perp = (\mathbf{Id} - \mathbf{e}\otimes\mathbf{e})\,\mathbf{d}\,. \tag{22}$$

Finally, it is interesting to notice that, since the axis of body rotation $\mathbf{R}$ is also the screw axis of the helix traced by the cell body, as the cell moves in average along the screw axis, the body rotates so that the lateral surfaces containing the eyespot (in which a light receptor is located) would be periodically exposed to or shaded from light, unless the screw axis is aligned with the light source. In fact, this could be a vivid example of a general biochemical mechanisms, repeatedly found in nature, to use periodic signals as a means to navigate in the sense that the existence of a periodic signal implies lack of alignment Goldstein (2015). The coupling between direction of average motion and axis of body rotations could explain the navigation mechanism used by phototactic Euglena to orient with a light source.

The result contained in the Helix Theorem is interesting in its universality, and it has far reaching consequences for the swimming of flagellated and ciliated unicellular organism: They all trace helical trajectories. In fact, the recent literature abounds with reports of discoveries of the helical structure of experimentally observed trajectories of a variety of micro-swimmers of great biological relevance (bacteria, sperm cells, etc.). Most of the previous literature had focused on the special cases of straight and circular trajectories, which are easily measured from two-dimensional images from an optical microscope, while the reconstruction of trajectories such as helices, which are spatial curves, require that we resolve the third dimension perpendicular to the focal plane of a microscope.

The interest and applications of the Helix Theorem above are not confined to trajectories of biological (and, possibly, artificial) micro-swimmers. Indeed, the theorem characterises the geometry of any chain resulting from the assembly of rigid monomers, when the position and orientation of the $(k+1)$-th monomer are constrained to be those arising from a shift $\mathbf{d}$ and a rotation $\mathbf{R}$ of the k-th one. The theorem shows that, in this case, a discrete circular helix will emerge. Enforcing that two monomers can only bind in a precise relative position and orientation is then a principle by which polymeric helical structures can self-assemble. This simple observation provides a rationale explaining why helices are so ubiquitous in Biology and Nature.

6. Conclusions and outlook

We have reviewed here some recent results on the fluid dynamics of unicellular swimmers. Most of our arguments have emphasised overarching conceptual principles, that can be used to rationalise complex biological behaviour. In view of their generality and far reaching nature, these principles are best discussed using the simplest system exhibiting the targeted level of complexity. It would be however misleading not to stress the key role that numerical simulation of the flows generated by micro-swimmers can play in the future developments of the field. This is true in at least two main directions.

The first one is in resolving the fine details of the induced flows, and capturing effects that are beyond the reach of simple models. This is already advocated in Arroyo et al. (2012), where the need of resolving the flows in the interior of the organism is apparent. Another interesting and quite unexplored issue is to assess the role of inertial effects associated with the pulsatile nature of flows generated by a fast beating flagellum, which moves in close proximity of the cell body.

ACCEPTED MANUSCRIPT

The details of these flows, the forces that they induce are often crucial to understand, for example, how microorganisms feed (driving food to their mouths), how they sense and respond to the environment (currents, density gradients of particles and chemicals, presence of other organisms and physical obstacles, etc.). Here, numerical simulation of biological fluid-structure interaction problems, coupled with experimental testing of their predictions through micro-velocimetry measurements, an approach pioneered in Drescher et al. (2010), will be extremely valuable.

In addition, as the field of bio-inspired micro-robots moves from the stage of intellectual speculation and proof-of-principle to the actual design of devices for biomedical applications, see Ornes (2017), the need for quantitatively accurate tools to move and steer micro-robots to their destinations, to model them and predict their behaviour is becoming acute, see Giuliani et al. (2018). Progress in this area will rely crucially on the development of agile and reliable tools for the prediction and control of motion, trajectories, and behaviour of these new bio-inspired micro-machines.

Acknowledgments

We gratefully acknowledge the support by the European Research Council through the ERC Advanced Grant 340685-MicroMotility. ADS thanks F. Alouges and M. Tucsnak for valuable discussions, the first related to recognising that the traveling bending waves of Section 4.2 represent an instance of the "No looping? No party!" locomotion principle, the second leading to the realisation that the Helix Theorem of Section 5.2 applies to periodic ciliar propulsion just as well as to flagellar propulsion.

References

References

Alouges, F., DeSimone, A., Lefebvre, A., 2008. Optimal strokes for low Reynolds number swimmers: an example. Journal of Nonlinear Science 18, 277–302.

Arroyo, M., DeSimone, A., 2014. Shape control of active surfaces inspired by the movement of euglenids. J. Mech. Physics Solids 62, 99–112. doi:10.1016/j.jmps.2013.09.017.

Arroyo, M., Milan, D., Heltai, L., DeSimone, A., 2012. Reverse engineering the euglenoid movement. Proc. Nat. Acad. Sciences USA 109, 17874–17879.

Carroll, D., Hankins, E., Kose, E., Sterling, I., 2014. A survey of the differential geometry of discrete curves. The Mathematical Intelligencer 36, 28–35.

Cicconofri, G., DeSimone, A., 2016. Motion planning and motility maps for flagellar microswimmers. Eur. Phys. J. E 39, 72. doi:10.1140/epje/i2016-16072-y.

Cohen, J., 2004. Mathematics is Biology's next microscope, only better; Biology is Mathematics' next Physics, only better. PLoS Biology 2, e439. doi:10.1371/journal.pbio.0020439.

Dal Maso, G., DeSimone, A., Morandotti, M., 2011. An existence and uniqueness result for the motion of self-propelled micro-swimmers. SIAM J. Math. Anal. 43, 1345–1368.

Drescher, K., Goldstein, R., Michel, N., Polin, M., Duval, I., 2010. Direct measurement of the flow field around swimming microorganisms. Physical Review Letters 105, 168101.

ACCEPTED MANUSCRIPT

Feynman, R., 1960. There's plenty of room at the bottom: An invitation to enter a new field of Physics. Engineering and Science 23, 22–36.

Gaffney, E., Gadelha, H., Smith, D., Blake, J., Kirkman-Brown, J., 2011. Mammalian sperm motility: Observation and theory. Annu. Rev. Fluid Mech. 43, 501–528.

Giuliani, N., Heltai, N., DeSimone, A., 2018. Predicting and optimizing micro-swimmer performance from the hydrodynamics of its components: the relevance of interactions. Soft Robotics doi:10.1089/soro.2017.0099.

Goldstein, R., 2015. Green algae as model organisms for biological fluid dynamics. Annu. Rev. Fluid Mech. 47, 343–375.

Guasto, J., Johnson, K., Gollub, J., 2010. Oscillatory flows induced by microorganisms swimming in two dimensions. Physical Review Letters 105, 168102.

Guasto, J., Rusconi, R., Stoker, R., 2012. Fluid mechanics of planktonic microorganisms. Annu. Rev. Fluid Mech. 44, 373–400.

Lauga, E., Powers, T.R., 2009. The hydrodynamics of swimming microorganisms. Reports on Progress in Physics 72, 096601.

Leander, B., Lax, G., Karnkowska, A., Simpson, A., 2017. Euglenida. Handbook of the protists doi:10.1007/978-3-319-32669-6_13-1.

Montino, A., DeSimone, A., 2015. Three-sphere low-Reynolds-number swimmer with a passive elastic arm. The European Physical Journal E 38, 1–10.

Najafi, A., Golestanian, R., 2004. Simple swimmer at low Reynolds number: Three linked spheres. Physical Review E 69, 062901.

Noselli, G., Beran, A., Arroyo, M., DeSimone, A., 2018. Theoretical and experimental study of metaboly in euglena gracilis. In preparation .

Ornes, S., 2017. Medical microrobots have potential in surgery, therapy, imaging, and diagnostics. Proc. Nat. Acad. Sciences USA 114, 12356–12358.

Purcell, E.M., 1977. Life at low Reynolds number. Am. J. Phys 45, 3–11.

Rossi, M., Cicconofri, G., Beran, A., Noselli, G., DeSimone, A., 2017. Kinematics of flagellar swimming in euglena gracilis: Helical trajectories and flagellar shapes. Proceedings of the National Academy of Sciences USA 114, 13085–13090. doi:10.1073/pnas.1708064114.

Shapere, A., Wilczeck, F., 1989. Geometry of self-propulsion at low Reynolds number. Journal of Fluid Mechanics 198, 557–585.

Taylor, G.I., 1951. Analysis of the swimming of microscopic organisms. Proceedings of the Royal Society of London A: Mathematical, Physical and Engineering Sciences 209, 447–461.

ACCEPTED MANUSCRIPT